

Organic & Biomolecular Chemistry

Accepted Manuscript



This is an *Accepted Manuscript*, which has been through the Royal Society of Chemistry peer review process and has been accepted for publication.

Accepted Manuscripts are published online shortly after acceptance, before technical editing, formatting and proof reading. Using this free service, authors can make their results available to the community, in citable form, before we publish the edited article. We will replace this *Accepted Manuscript* with the edited and formatted *Advance Article* as soon as it is available.

You can find more information about *Accepted Manuscripts* in the [Information for Authors](#).

Please note that technical editing may introduce minor changes to the text and/or graphics, which may alter content. The journal's standard [Terms & Conditions](#) and the [Ethical guidelines](#) still apply. In no event shall the Royal Society of Chemistry be held responsible for any errors or omissions in this *Accepted Manuscript* or any consequences arising from the use of any information it contains.

Cite this: DOI: 10.1039/c0xx00000x

ARTICLE TYPE

www.rsc.org/xxxxxx

Characterizations of cationic γ -carbolines binding with double-stranded DNA by spectroscopic methods and AFM imaging

Tao Jia ^{a*}, Jing Wang ^b, Peng Guo ^a, Junping Yu ^{b*}

Received (in XXX, XXX) Xth XXXXXXXXXX 20XX, Accepted Xth XXXXXXXXXX 20XX

DOI: 10.1039/b000000x

Two cationic γ -carbolines, 2-methyl-5*H*-pyrido[4,3-*b*]indolium iodide (**MPII**) and 2,5-Dimethyl-5*H*-pyrido[4,3-*b*]indolium iodide (**DPII**), were synthesized, and the DNA binding properties of the cationic γ -carbolines were elucidated. Through a series of experiments, we proved that the two cationic γ -carbolines could strongly interact with DNA by intercalative binding. However, **DPII**, with a methyl group substituting H atom of 5-NH, has shown a stronger intercalative interaction with DNA than **MPII**. The dissociation of H from 5-NH of **MPII** resulted in a better water-solubility and less binding affinity to DNA. Atomic force microscopy (AFM) images of pBR322 showed that both **MPII** and **DPII** strongly interacted with DNA and induced conformational changes of DNA. Meanwhile, the CT-DNA circular dichroism (CD) spectra changes and the statistics of node numbers of pBR322 in AFM images indicated that **MPII** had more profound effects on DNA conformations than **DPII**. Furthermore, our studies have shown the interactions between cationic γ -carbolines and DNA were sensitive to ionic strength. Increased ionic strength in the buffer prompted the DNA helix to shrink, and the base stacking would be more compact, which resulted in hardly intercalating of cationic γ -carbolines into DNA.

Introduction

DNA is an important target of anti-cancer or anti-microbial drug designs. As well the interactions between DNA and small molecular ligands, especially the structural variations of DNA on ligand-binding, are of great significance in biology and medicine. The interactions between small molecular ligands and DNA might be intercalation, or groove binding, and the structure of DNA-interacting molecules and the nature of DNA decide the interaction preferences. Small differences in the structure of a DNA-interacting molecule may affect the binding types and stability of the molecule/DNA complex.^{1,2}

Planar and aromatic moieties would contribute to intercalative interactions between small molecules and DNA, where the moieties can slide between the adjacent base pairs and be in favour of the intercalation.³ Carbolines with characteristic polycyclic planar aromatic nucleus have drawn an increasing attention. Among these carbolines of various structures, β -carbolines are a group of alkaloids found in numerous plants⁴ and mammal organism⁵, and have lately been subjected to intensive study in many biological processes, whereas their α - and γ -analogs have been relatively neglected. β -Carbolines have been reported to be a class of potential antitumor agents, which showed their antitumor activity through multiple mechanisms, such as intercalating into DNA⁶⁻⁸, inhibiting topoisomerase I and II⁹⁻¹¹, Cyclin-Dependent Kinase (CDK)¹²⁻¹⁴ and Polo-like-kinase (PLK)^{15,16}. Compared with the studies of β -carbolines, the biological study of differently structural carbolines is poor.

The intercalative binding of β -carbolines with DNA have been proved strong dependence on pH, and the protonated forms of β -carbolines (βCsH^+) showed a higher interaction than the neutral forms^{6,17}, which is thought that the positive charge in the chromophore is essential for increasing their DNA affinity¹⁸. Meanwhile, the effect of ionic strength is of importance in the interaction between β -carbolines and DNA, the increasing of ionic strength of the medium weakens the electrostatic attraction between a positive charged β -carbolines and DNA.⁷ After intercalative binding to DNA, β -carbolines could induce DNA photocleavage *via* a type I mechanism.^{6-8,17}

However, little information was obtained about the DNA-binding of γ -carbolines. In our recent work, γ,γ' -diazacarbazole dication (**DPDI**) has been proved to interact with DNA by intercalation and groove binding, and the DNA binding properties were sensitive to ionic strength.¹ In groove interactions, dications of 3,6-dipyridinium on **DPDI** interacted with DNA base pairs to closely fit the helical twist of the groove, and -NH on pointed out of the groove.¹ To find more efficient intercalating agents, the DNA binding properties of γ -carboline cations to DNA have been studied here.

In this study, cationic γ -carboline, 2-Methyl-5*H*-pyrido[4,3-*b*]indolium iodide (**MPII**) have been synthesized and characterized. Through fluorescence titrations and absorption titrations, the strong interactions with DNA have been confirmed. However, whether -NH on **MPII** participated in the interactions between **MPII** and DNA was not clear. In order to clarify this question and the interaction preferences between **MPII** and DNA, another cationic γ -carboline derivative, where a methyl group was utilized to block -NH on **MPII**, 2,5-Dimethyl-5*H*-

pyrido[4,3-*b*]indolium iodide (**DPII**, the structure is illustrated in Fig. 1.), was synthesized and characterized. The spectral titrations of both **MPII** and **DPII** with CT-DNA including UV-Vis absorption and fluorescence revealed that both compounds had high affinities to DNA. The CD spectra, ethidium bromide (EB) competitions and H33258 competitions disclosed that both compounds interacted with DNA by intercalations, and EB competitions and H33258 competitions indicated that **DPII** showed a higher intercalating activity than **MPII**. Moreover, both **MPII** and **DPII** induced conformational compression of DNA, as demonstrated by atomic force microscopy (AFM). The studies on the interactions between cationic γ -carbolines and DNA would broaden the understandings and applications of γ -carbolines as DNA structural probes or as cancer therapeutics targeted to DNA.

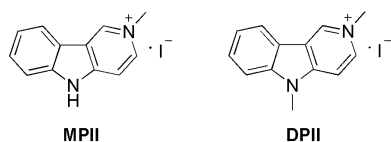


Fig. 1. The structures of **MPII** and **DPII**.

Results and discussion

Fluorescence titration

In the fluorescent experiment, we found that both **MPII** and **DPII** have similar fluorescent properties. During the experiments, fluorescence decay over time was hardly observed. And increasing ionic strength of the medium resulted in fluorescence enhancement of both cationic γ -carbolines, although only small increase of fluorescence was observed.

Fluorescence titration of γ -carbolines with CT-DNA was applied to investigate the binding properties of **MPII/DPII** with DNA. Fig. 2-1 and 2-2 illustrate the fluorescence changes of **MPII** and **DPII**, respectively, by titration of CT-DNA at various ionic strengths.

Fluorescence quenching of cationic γ -carbolines by DNA was observed at various ionic strengths. As ionic strength increased, fluorescence quenching was lessening gradually, where maximal quenching was varied from 33.4 % to 17.8 % for **MPII** and from 47.9 % to 17.2 % for **DPII** under same additional DNA concentration. The corresponding relative fluorescence intensity decreases with the titration of **MPII** and **DPII** by CT-DNA were exhibited in ESI Fig. S1.

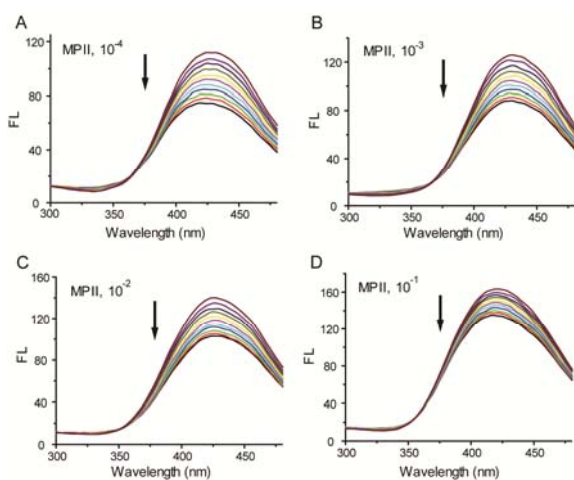


Fig.2-1. Fluorescence emission changes when titration of **MPII** by CT-DNA. [**MPII**] = 0.1 μ M in buffer of pH=7.4; [DNA base pairs] = 0, 1.02, 2.04, 3.06, 4.08, 5.10, 6.12, 7.14, 8.16, 9.18, 10.20 μ M. (A) buffer (1.0 \times 10⁻⁴ M Tris-HCl, 1.0 \times 10⁻⁴ M NaCl); (B) buffer (1.0 \times 10⁻³ M Tris-HCl, 1.0 \times 10⁻³ M NaCl); (C) buffer (1.0 \times 10⁻³ M Tris-HCl, 1.0 \times 10⁻² M NaCl); (D) buffer (1.0 \times 10⁻³ M Tris-HCl, 1.0 \times 10⁻¹ M NaCl).

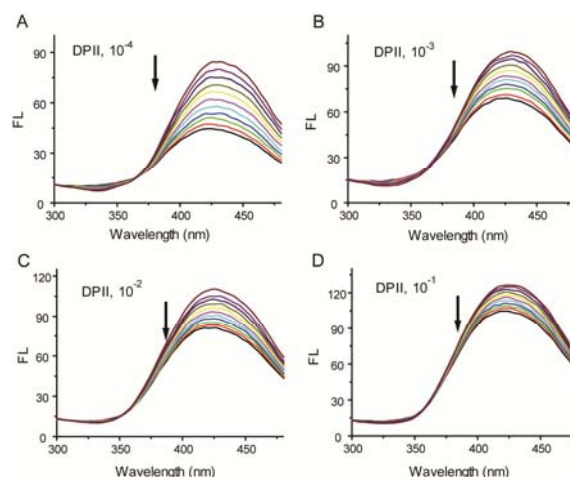


Fig. 2-2. Fluorescence emission changes when titration of **DPII** by CT-DNA. [**DPII**] = 0.1 μ M in buffer of pH=7.4; [DNA base pairs] = 0, 1.02, 2.04, 3.06, 4.08, 5.10, 6.12, 7.14, 8.16, 9.18, 10.20 μ M. (A) buffer (1.0 \times 10⁻⁴ M Tris-HCl, 1.0 \times 10⁻⁴ M NaCl); (B) buffer (1.0 \times 10⁻³ M Tris-HCl, 1.0 \times 10⁻³ M NaCl); (C) buffer (1.0 \times 10⁻³ M Tris-HCl, 1.0 \times 10⁻² M NaCl); (D) buffer (1.0 \times 10⁻³ M Tris-HCl, 1.0 \times 10⁻¹ M NaCl).

Fluorescence changing (increasing or decreasing) is a criterion for the interactions between small molecules and DNA, and the extent of fluorescence quenching is corresponding to the strength of interactions.¹⁹ The fluorescence of either cationic γ -carboline was greatly quenched by DNA, which indicated the strong interactions between cationic γ -carbolines and DNA. The interactions were weakened with ionic strength increasing. At low ionic strength, the stronger fluorescence quenching for **DPII** by DNA titration than **MPII** indicated the stronger interactions between **DPII** and DNA than those between **MPII** and DNA.

UV-Vis absorption titration

Red shift and hypochromism in absorption spectra of small molecules upon binding with DNA have been commonly used to characterize the interactions between small molecules and DNA. It was generally accepted that the extent of the hypochromism was consistent with the strength of the interactions.

Because the solubility of **DPII** was not good in aqueous solutions, DMSO was used as a solvent for preparing stock solution, while DMSO disturbed UV-Vis detection to some extent at short wavelength close to 210 nm. Therefore, UV-Vis absorption titration of **DPII** by CT-DNA was recorded from 240 to 350 nm. The absorption spectra of **MPII** and **DPII** titrated by CT-DNA were illustrated in Fig. 3-1 and Fig. 3-2, respectively. Both DNA and cationic γ -carbolines have strong UV-Vis absorption, so a reference cuvette contained corresponding CT-DNA alone to nullify the negative control absorbance.

At low ionic strength of 10⁻⁴ M, titrations of CT-DNA into **MPII** caused spectral changes dramatically. Two major absorption peaks (213 and 260 nm) of **MPII** exhibited apparent hypochromicity, with the maxima of 35.9 % at 213 nm and 50.1 % at 260 nm. Moreover, an obvious red shift of the peak from 213 nm to 220 nm was observed. With ionic strength increasing, hypochromic effect decreased gradually and almost disappeared at 10⁻¹ M.

Similarly, apparent hypochromism of **DPII** by DNA titration was observed, and the extent of hypochromic effect was relative to ionic strength. At low ionic strength of 10⁻⁴ M, the major

absorption peak (262 nm) of **DPII** exhibited an apparent hypochromicity, with the maximum of 65.9 % at 262 nm. The hypochromic effect in **DPII** titration was stronger than that in **MPII** titration under same additional DNA concentration, indicating the stronger interactions between **DPII** and DNA than those between **MPII** and DNA, which were consistent with the results obtained from fluorescence titration. The corresponding relative UV-Vis absorbance decreases with the titration of **MPII** and **DPII** by CT-DNA were exhibited in ESI Fig. S2.

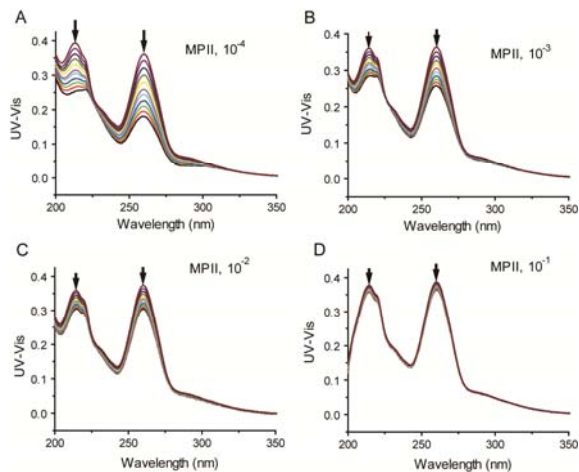


Fig.3-1 UV-Vis absorbance changing with the titration of **MPII** by CT-DNA. [**MPII**] = 10 μM in buffer of pH=7.4; [DNA base pairs] = 0, 3.58, 7.16, 10.74, 14.32, 17.90, 21.48, 25.06, 28.64, 32.22, 35.80 μM. (A) buffer (1.0 × 10⁻⁴ M Tris-HCl, 1.0 × 10⁻⁴ M NaCl); (B) buffer (1.0 × 10⁻³ M Tris-HCl, 1.0 × 10⁻³ M NaCl); (C) buffer (1.0 × 10⁻² M Tris-HCl, 1.0 × 10⁻² M NaCl); (D) buffer (1.0 × 10⁻¹ M Tris-HCl, 1.0 × 10⁻¹ M NaCl).

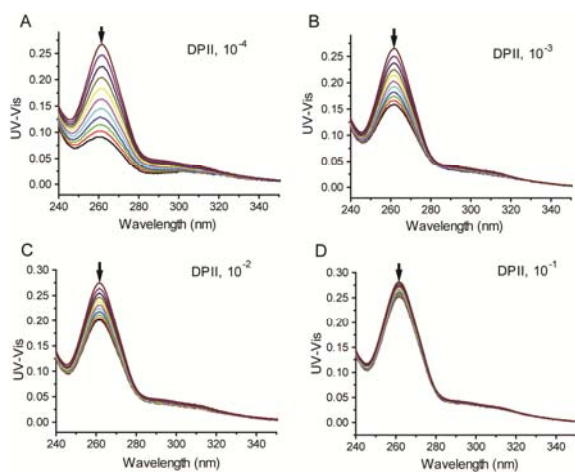


Fig.3-2 UV-Vis absorbance changing with the titration of **DPII** by CT-DNA. [**DPII**] = 10 μM in buffer of pH=7.4; [DNA base pairs] = 0, 3.58, 7.16, 10.74, 14.32, 17.90, 21.48, 25.06, 28.64, 32.22, 35.80 μM. (A) buffer (1.0 × 10⁻⁴ M Tris-HCl, 1.0 × 10⁻⁴ M NaCl); (B) buffer (1.0 × 10⁻³ M Tris-HCl, 1.0 × 10⁻³ M NaCl); (C) buffer (1.0 × 10⁻² M Tris-HCl, 1.0 × 10⁻² M NaCl); (D) buffer (1.0 × 10⁻¹ M Tris-HCl, 1.0 × 10⁻¹ M NaCl).

From absorption spectral titration data, the intrinsic binding constant K_b for carbolines/DNA can be calculated using the following equation:

$$[DNA] / (\epsilon_f - \epsilon_a) = [DNA] / (\epsilon_f - \epsilon_b) + 1 / K_b (\epsilon_f - \epsilon_b)$$

where [DNA] is the concentration of DNA in base pairs and ϵ_a , ϵ_b , ϵ_f respectively correspond to the apparent absorption coefficient A/[carbolines], the extinction coefficient for the free compound and the extinction coefficient of the compound when

fully bound to DNA. From the slope and intercept of the plot $[DNA] / (\epsilon_f - \epsilon_a)$ vs. [DNA], K_b can be obtained.²¹

The K_b values were listed in table 1. The corresponding fitting figures were shown in ESI Fig. S3. The intrinsic binding constant K_b for carbolines/DNA decreased with increasing the ionic strength, and K_b of **MPII**/DNA was greater than that of **DPII**/DNA, at respective ionic strength (except in the ionic strength of 10⁻¹ M).

The linear fittings in the ionic strength of 10⁻¹ M were not very good (as shown in Fig. S3D and H), probably because the binding strengths in the ionic strength of 10⁻¹ M were weak.

Table 1. The K_b values of different complex formed by carbolines and DNA at different ionic strengths.

ionic strength	K_b of MPII /DNA	K_b of DPII /DNA
10 ⁻¹ M	(7.72 ± 1.54) × 10 ⁷ M ⁻¹	(4.09 ± 0.52) × 10 ⁷ M ⁻¹
10 ⁻³ M	(1.97 ± 0.12) × 10 ⁷ M ⁻¹	(1.49 ± 0.75) × 10 ⁷ M ⁻¹
10 ⁻² M	(6.86 ± 0.25) × 10 ⁶ M ⁻¹	(6.43 ± 0.48) × 10 ⁶ M ⁻¹
10 ⁻¹ M	(6.96 ± 1.24) × 10 ⁵ M ⁻¹	(1.52 ± 0.35) × 10 ⁶ M ⁻¹

Circular dichroism spectroscopy

CD spectroscopy (Circular Dichroism) are generally utilized to characterized the binding of small molecules to DNA, and the changes of DNA conformations can be ascribed to the observed changes of DNA CD signals.²² The characteristic CD spectrum of CT-DNA in the region 220-320 nm could provide the information relevant to structural changes on DNA upon interactions with cationic γ -carbolines. Fig. 4-1 and 4-2 depicted the CD spectra of CT-DNA with increasing concentrations of **MPII** and **DPII**, respectively, at various ionic strengths. Because DMSO disturbed CD detection beneath 230 nm, CD spectrum of CT-DNA upon interactions with **DPII** was recorded in the region 230-320 nm.

The typical B-form of free CT-DNA would show a positive Cotton effect near 275 nm because of base stacking and a negative Cotton effect near 245 nm due to right-handed helicity, on CD spectra of CT-DNA.²² It is generally accepted that the classical intercalations between small molecules and CT-DNA would enhance the base stacking and stabilize the right-handed helicity, and thus increase the positive band, while groove binding and electrostatic interactions would reveal less or no disturbance on the above two bands.²³

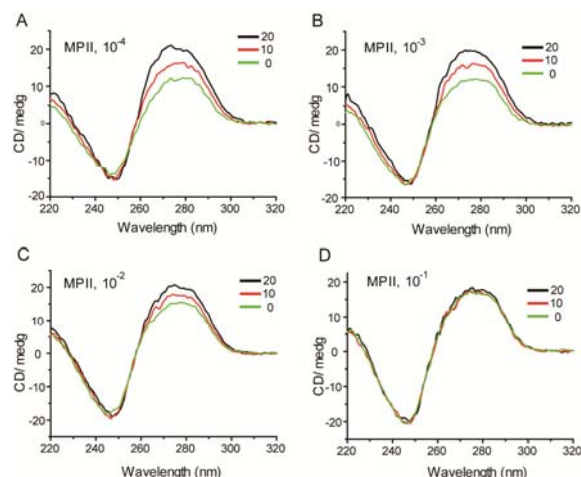


Fig. 4-1. CD spectra of CT-DNA (100 μM) at increasing **MPII** concentration (0, 10, 20 μM). (A) buffer (1.0 × 10⁻⁴ M Tris-HCl, 1.0 × 10⁻⁴ M NaCl); (B) buffer (1.0 × 10⁻³ M Tris-HCl, 1.0 × 10⁻³ M NaCl); (C) buffer (1.0 × 10⁻² M Tris-HCl, 1.0 × 10⁻² M NaCl); (D) buffer (1.0 × 10⁻¹ M Tris-HCl, 1.0 × 10⁻¹ M NaCl).

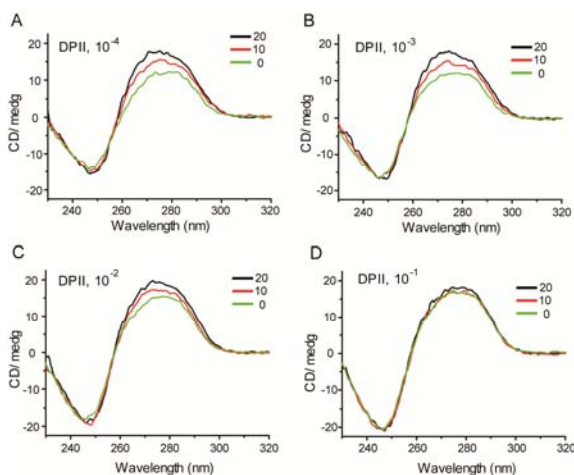


Fig. 4-2. CD spectra of CT-DNA (100 μM) at increasing **DPII** concentration (0, 10, 20 μM). (A) buffer (1.0×10⁻⁴ M Tris-HCl, 1.0×10⁻⁴ M NaCl); (B) buffer (1.0×10⁻³ M Tris-HCl, 1.0×10⁻³ M NaCl); (C) buffer (1.0×10⁻³ M Tris-HCl, 1.0×10⁻² M NaCl); (D) buffer (1.0×10⁻³ M Tris-HCl, 1.0×10⁻¹ M NaCl).

Almost all figures revealed an enhancement of the positive band in the CD signal of CT-DNA with increasing concentration of cationic γ -carbolines, which was rationalized on the intercalations of cationic γ -carbolines to DNA base pairs enhancing the base stacking. And with ionic strength increasing, the increase in the positive band intensity at 275 nm decreased gradually and almost disappeared at ionic strength of 10⁻¹ M, which suggested that high ionic strength could prevent the intercalative binding of cationic γ -carbolines to CT-DNA.

In analogy to our reported work, a new positive band at 260-270 nm was manifested to be a result of the groove interaction.¹ But it was not observed in the CD signal of CT-DNA upon the interaction with either **MPII** or **DPII**, indicating that groove interactions do not exist between cationic γ -carbolines and DNA.

At ionic strength of 10⁻⁴ M, the intensity of the positive band at 275 nm increased with the maximum of 77.9% for **MPII** and 57.3% for **DPII**. At ionic strength of 10⁻³ M, the intensity of the positive band at 275 nm increased with the maximum of 67.7% for **MPII** and 50.9% for **DPII**. These phenomena indicated that **MPII** had more profound effects on DNA conformations than **DPII**, which was consistent with the following AFM results. While with ionic strength increasing, the enhancement of the positive band at 275 nm by **MPII** is almost same to that of **DPII** additions.

EB and H33258 competitive experiments

EB is a classical intercalator of DNA and H33258 is a representative DNA-groove binder.²⁴ To further confirm the interaction modes of cationic γ -carbolines with DNA and analyse the binding strength of interaction between cationic γ -carbolines and DNA, experiments of EB and H33258 competitive binding to DNA were carried out by the fluorescence spectra at various ionic strengths.

In EB competitive experiments, it was hard for **MPII** to replace EB from the complex of EB-DNA, and only relative small decrease of original fluorescence of EB-DNA at various ionic strengths was shown in Fig. 5-1. Meanwhile, ionic strength also affected original fluorescence of EB-DNA complex, and high ionic strength impeded the interaction between EB and DNA.

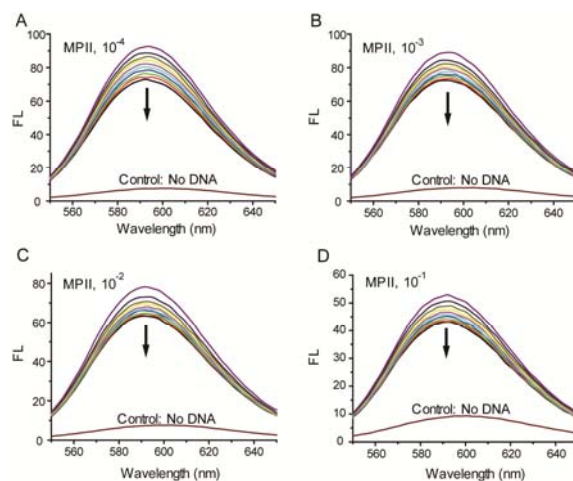


Fig. 5-1. Fluorescence spectra of EB (2 μM) and DNA (5 μM) with the increasing addition of **MPII**. [**MPII**] = 0, 3.33, 6.67, 10.00, 13.33, 16.67, 20.00, 23.33, 26.67, 30.00 μM. (A) buffer (1.0×10⁻⁴ M Tris-HCl, 1.0×10⁻⁴ M NaCl); (B) buffer (1.0×10⁻³ M Tris-HCl, 1.0×10⁻³ M NaCl); (C) buffer (1.0×10⁻³ M Tris-HCl, 1.0×10⁻² M NaCl); (D) buffer (1.0×10⁻³ M Tris-HCl, 1.0×10⁻¹ M NaCl).

On the contrary, the fluorescence of EB-DNA complex was decreasing rapidly with the addition of **DPII**. 30 μM **DPII** could quench the fluorescence of EB-DNA complex from 48% to 80% with ionic strength increasing, as showed as Fig. 5-2. The phenomena indicated that **DPII** could compete for the binding site of DNA upon EB intercalation and release EB from EB-DNA complex. Moreover, the results revealed that the fluorescence of EB-DNA was affected by **DPII** more apparently at high ionic strength than that at low ionic strength. We can describe to that with the ionic strength increasing, the bind affinity of EB-DNA complex weakened, which resulted in the dissociation of EB-DNA complex upon **DPII** intercalation to DNA, thus leading to the high quenching effect of **DPII** on EB-DNA complex at high ionic strength. The EB competitive experiments of cationic γ -carbolines indicated that **DPII** showed the stronger intercalation to DNA than **MPII** did. The corresponding relative fluorescence intensity decreases with the titration of EB-DNA by **MPII** and **DPII** were exhibited in ESI Fig. S4.

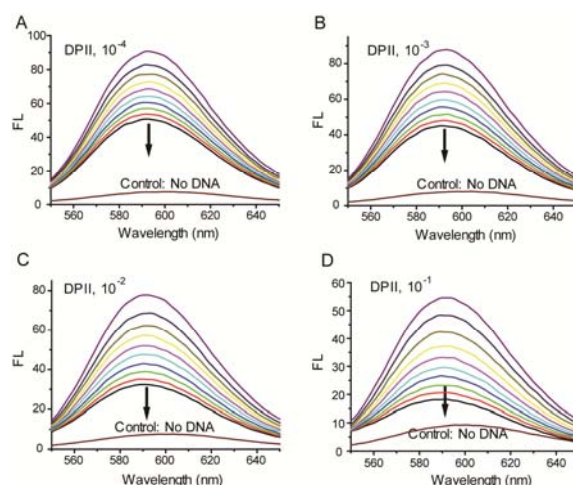


Fig. 5-2. Fluorescence spectra of EB (2 μM) and DNA (5 μM) with the increasing addition of **DPII**. [**DPII**] = 0, 3.33, 6.67, 10.00, 13.33, 16.67, 20.00, 23.33, 26.67, 30.00 μM. (A) buffer (1.0×10⁻⁴ M Tris-HCl, 1.0×10⁻⁴ M NaCl); (B) buffer (1.0×10⁻³ M Tris-HCl, 1.0×10⁻³ M NaCl); (C) buffer (1.0×10⁻³ M Tris-HCl, 1.0×10⁻² M NaCl); (D) buffer (1.0×10⁻³ M Tris-HCl, 1.0×10⁻¹ M NaCl).

H33258 competitive results were shown in Fig. 6-1 and 6-2. The corresponding relative fluorescence intensity decreases with the titration of H33258-DNA by **MPII** and **DPII** were exhibited in ESI Fig. S5. Although the original fluorescence of H33258-DNA complex was decreasing with the addition of **MPII** or **DPII**, an end point of titration always existed, which was different from EB competitive results. These phenomena indicated that the binding mode of cationic γ -carbolines to DNA was intercalation, which was different from that of H33258 to DNA. The intercalation of cationic γ -carbolines to DNA made DNA morphology change and to release a fraction of H33258 from H33258-DNA complex. When all binding sites for intercalation were occupied by cationic γ -carbolines, more cationic γ -carbolines would not induce releasing H33258 from H33258-DNA complex and thus no decrease the fluorescence of H33258-DNA complex, and a further change of the fluorescence resulted from cationic γ -carbolines addition. At ionic strength of 10^{-2} M, only a little decreases the fluorescence of H33258-DNA complex were observed. At ionic strength of 10^{-1} M, the addition of **MPII** or **DPII** would increase the fluorescence of the system, which resulted from the fluorescence of cationic γ -carbolines. Thus, the experiments at 10^{-1} M were omitted.

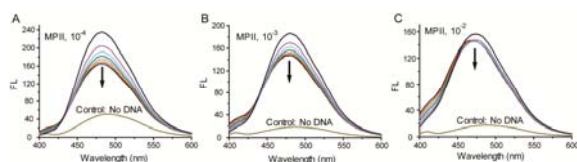


Fig. 6-1. Fluorescence spectra of H33258 (2 μ M) and DNA (5 μ M) with the increasing addition of **MPII**. [**MPII**] = 0, 3.33, 6.67, 10.00, 13.33, 16.67, 20.00 μ M. (A) buffer (1.0×10^{-4} M Tris-HCl, 1.0×10^{-4} M NaCl); (B) buffer (1.0×10^{-3} M Tris-HCl, 1.0×10^{-3} M NaCl); (C) buffer (1.0×10^{-3} M Tris-HCl, 1.0×10^{-2} M NaCl).

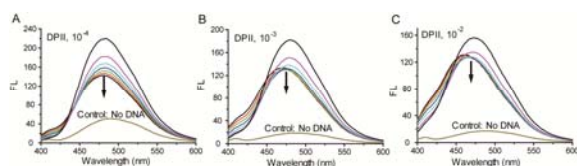


Fig. 6-2. Fluorescence spectra of H33258 (2 μ M) and DNA (5 μ M) with the increasing addition of **DPII**. [**DPII**] = 0, 3.33, 6.67, 10.00, 13.33, 16.67, 20.00 μ M. (A) buffer (1.0×10^{-4} M Tris-HCl, 1.0×10^{-4} M NaCl); (B) buffer (1.0×10^{-3} M Tris-HCl, 1.0×10^{-3} M NaCl); (C) buffer (1.0×10^{-3} M Tris-HCl, 1.0×10^{-2} M NaCl).

20 μ M **MPII** quenched the fluorescence of H33258-DNA complex for 42%, 23% and 8% at ionic strength of 10^{-4} , 10^{-3} and 10^{-2} M, respectively, while 20 μ M **DPII** quenched the fluorescence for 45%, 33% and 25%, respectively. The extent of the fluorescence quenching suggested the change extent of DNA morphology upon cationic γ -carbolines intercalation. Therefore, the intercalating interaction between **DPII** and DNA was stronger than that between **MPII** and DNA, which accorded with the results obtained from fluorescence titration, UV-vis titration and EB competitive experiments.

Effect of ionic strength

Cationic γ -carbolines carries a positive charge and DNA has a negatively charged polyphosphate backbone, so the effect of ionic strength on cationic γ -carboline-DNA binding interaction has been studied. The strong electrolyte NaCl has been employed to adjust the ionic strength in buffers and study the impact of electrostatic interaction on the interactions between cationic γ -carbolines and DNA.^{1,7}

Increased ionic strength in the buffer screens the electrostatic repulsion between consecutive phosphate groups, prompting the

helix to shrink.²⁵ The CD spectrum of free CT-DNA is of the typical B-form, with a positive Cotton effect near 275 nm due to base stacking and a negative Cotton effect near 245 nm due to right-handed helicity.²² Therefore, the effect of ionic strength was confirmed by the CD signal of CT-DNA, which increased ionic strength enhanced the positive Cotton effect near 275 nm and the negative Cotton effect near 245 nm simultaneously, as shown in Fig. 7 A.

At low ionic strengths (10^{-3} M and 10^{-4} M), similar strength of the positive Cotton effect indicated the similar electrostatic repulsion between consecutive phosphate groups. The intercalation of same concentration cationic γ -carbolines into DNA would enhance the base stacking and make the positive Cotton effect increase correspondingly, while the negative Cotton effect showed less perturbation, as seen in Fig. 4-1 A and B. With ionic strength increasing, the electrostatic repulsion between consecutive phosphate groups would decrease, and the base stacking would be more compact, which resulted in hardly intercalating of cationic γ -carbolines into DNA, as seen in Fig. 4-1 C and D.

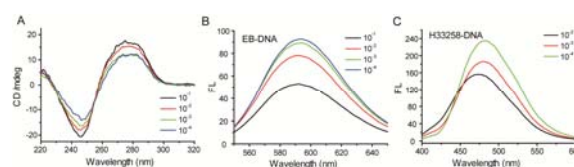


Fig. 7. CD spectra of CT-DNA (100 μ M) (A) at various ionic strength buffers; Fluorescence spectra of EB-DNA (2 μ M : 5 μ M) complex (B) and H33258-DNA (2 μ M : 5 μ M) complex (C) at various ionic strength buffers.

Meanwhile, the fluorescence change of fluorophore-DNA complex was also verified that an increase in ionic strength of buffer would affect the interaction between fluorophore and DNA, whether as intercalating agent or as groove binding agent. Fig. 7 B and C revealed the effect of ionic strength on the fluorescence properties of EB-DNA complex and H33258-DNA complex, respectively. As for EB-DNA complex, high ionic strengths impeded the interactions between EB and DNA, thus the original fluorescence of EB-DNA complex decreased with ionic strength increasing.

AFM imaging

To visualize the conformational changes of DNA induced by γ -carbolines at low ionic strength, AFM experiments were carried out at low ionic strength of about 10^{-3} M. Different cationic

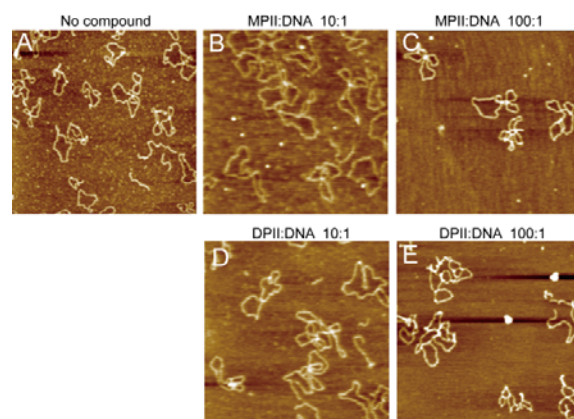


Fig. 8. AFM images for pBR322 with the increase of **MPII** and **DPII** at the mole ratio of compound:DNA=0:1 (A), 10:1 (B and D), 100:1 (C and E)). Scan area: 1500 nm \times 1500 nm. Z range is 2 nm.

γ -carbolines/pBR322 (bps) mixing mole ratios (0, 10:1, 100:1) were adopted for the AFM studies. The images were shown in Fig.8 with scan range 1500 nm \times 1500 nm. The phenomena observed by AFM were similar to previously reported results,²⁶ suggesting that both **MPII** and **DPII** strongly interacted with DNA and induced conformational changes of DNA at low ionic strength.

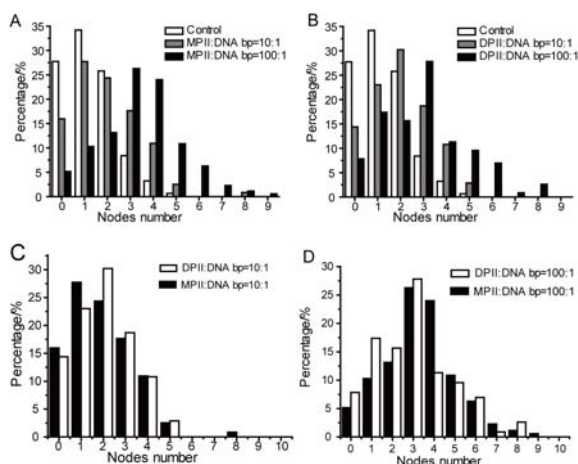


Fig. 9. DNA plasmid node number distribution as a function of different ratios of the two cationic γ -carbolines. (A) Node number distributions in the presence of different **MPII** concentrations. (B) Node number distributions in the presence of different **DPII** concentrations. (C) Node number distributions in the presence of **MPII** or **DPII**:DNA at the ratio of 10:1. (D) Node number distributions in the presence of **MPII** or **DPII**:DNA at the ratio of 100:1.

Statistics of node number of each pBR322 molecule can be adopted to look at the conformational changes in the presence of compounds.^{27,28} As shown in Fig. 9, with the increase of either of the two cationic γ -carbolines/pBR322 ratios, the node number distributions shifted to high values. Therefore, we can conclude that the conformations of pBR322 were changed and presented more supercoiled conformations. AFM data have shown more node numbers of pBR322 for **MPII** than for **DPII**, which demonstrated that **MPII** had more profound effects on DNA conformations than **DPII**. The results are consistent with the results of CD spectra and the binding constants K_b shown in table 1.

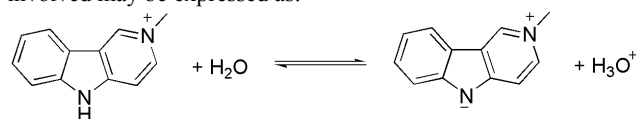
DNA binding properties of cationic γ -carbolines

Cationic γ -carbolines was planar aromatic molecules, which contributes to the intercalation of cationic γ -carbolines to DNA base pairs. The titrations of fluorescence and UV-Vis confirmed the strong interactions between cationic γ -carbolines and DNA. Except for intercalation, were more than one type of binding interaction involved in the interactions between cationic γ -carbolines and DNA? It was reported that -NH groups of the carbazoles substituted at 2,7 positions with cationic amidine groups or imidazoline groups bond strongly to the DNA groove of AT-rich sequences.^{29,30} We have reported that dications of pyridinium on 3,6-diazacarbazole could interact with DNA base pairs through groove binding, and -NH on 3,6-diazacarbazole points out of the groove.¹ By introducing a methyl group substituting H atom at -NH group of **MPII**, **DPII** was designed to clarify whether -NH participated to bind with DNA.

In the CD signal of CT-DNA upon interacting with **MPII**, there was no band of 260-270nm observed, indicating that groove interactions did not exist between cationic γ -carbolines and DNA, because the band at 260-270nm was ascribed to the groove

interaction.¹ Thus, 2-N-methylpyridinium cation and 5-NH of γ -carboline did not form a groove binding with DNA, which also was verified by EB/H33258 competitive experiments.

MPII showed a good water-solubility in preparing the stock solution, while **DPII** with a methyl group substituting H atom at 5-NH did not. All experiments confirmed that the intercalating interaction between **DPII** and DNA was stronger than that between **MPII** and DNA. And in EB competitive experiments, **DPII** not **MPII** could compete for the binding site of DNA upon EB intercalation and release EB from EB-DNA complex. The different binding activities of cationic γ -Carbolines with DNA were due to the similarity and difference in the structures between **MPII** and **DPII**. γ -Carboline methiodide (**MPII**) showed a little alkaline by the dissociation of H from 5-NH.³¹ The equilibrium involved may be expressed as:



The dissociation of H from 5-NH of **MPII** could interpret the water-solubility, and also explain the less intercalating interaction to DNA than **DPII**. The H-dissociated **MPII**, which was equal to an electroneutral molecule, has shown lower binding affinity to DNA than **DPII** with a positive charge. But when dissociated **MPII** intercalated into DNA bases, the electroneutral **MPII** would decrease the electrostatic interaction between intercalating reagent and DNA bases, which might induce greater conformational change of DNA than cationic **DPII**. Both CD signal of CT-DNA and the statistics of node numbers of pBR322 with cationic γ -carbolines proved it.

Experimental Section

Synthesis

2-Methyl-5H-pyrido[4,3-b]indolium iodide (**MPII**)

A mixture of γ -carboline (60 mg, 0.357 mmol) and iodomethane (0.5 mL, 8.03 mmol) in ethanol (6 mL) was stirred and heated to 60 °C in a sealed tube for 24 h. Then the excess iodomethane and ethanol were removed under reduced pressure, and the residue was recrystallized from ethanol to give pale yellow powders 85 mg, Yield: 77%. ¹H NMR (DMSO-*d*₆) δ : 4.38 (s, 3H, CH₃), 7.52 (t, *J* = 7.5 Hz, 1H, H₈), 7.72 (t, *J* = 7.6 Hz, 1H, H₇), 7.80 (d, *J* = 8.1 Hz, 1H, H₆), 8.04 (d, *J* = 6.9 Hz, 1H, H₉), 8.37 (d, *J* = 7.9 Hz, 1H, H₄), 8.68 (d, *J* = 6.8 Hz, 1H, H₃), 9.83 (s, 1H, H₁), 13.07 (s, 1H, NH); ¹³C NMR (DMSO-*d*₆) δ : 46.65, 108.57, 113.11, 120.03, 120.09, 121.81, 122.64, 129.48, 139.02, 139.21, 141.31, 144.96; HRMS (ESI) *m/z* calcd for C₁₂H₁₁N₂ [M-I]⁺ 183.0922, found 183.0922.

2-Methyl-2H-pyrido[4,3-b]indole

In a mixture of CH₂Cl₂ (30 mL) and 28-30% ammonia in water (30 mL), 2-Methyl-5H-pyrido[4,3-b]indolium iodide (50 mg, 0.161 mmol) was added, then stirred over night. The organic phase was separated and the aqueous phase was subsequently extracted with CH₂Cl₂ (4 \times 20 mL). The combined organic phase was dried over MgSO₄, filtered and evaporated to dryness to afford pale yellow powders 25 mg, Yield: 85%. ¹H NMR (CDCl₃) δ : 4.06 (s, 3H, CH₃), 7.25 (t, *J* = 7.5 Hz, 1H, H₇), 7.44-7.49 (m, 2H, H₆, H₉), 7.54 (t, *J* = 7.6 Hz, 1H, H₈), 7.85 (d, *J* = 8.2 Hz, 1H, H₄), 7.97 (d, *J* = 7.8 Hz, 1H, H₃), 8.42 (s, 1H, H₁); ¹³C NMR (CDCl₃) δ : 45.67, 110.91, 117.50, 120.35, 120.43, 122.46,

122.83, 128.06, 132.91, 132.99, 151.90, 152.83; HRMS (ESI) m/z calcd for $C_{12}H_{11}N_2$ $[M+H]^+$ 183.0922, found 183.0930.

2,5-Dimethyl-5H-pyrido[4,3-b]indolium iodide (DPII)

A mixture of 2-methyl-2H-pyrido[4,3-b]indole (35 mg, 0.192 mmol) and iodomethane (0.5 mL, 8.03 mmol) in ethanol (6 mL) was stirred and heated to 60 °C in a sealed tube for 4 h. Then the excess iodomethane and ethanol were removed under reduced pressure, and the residue was recrystallized from ethanol to give black needles 35 mg, Yield: 56 %. 1H NMR (DMSO- d_6) δ : 4.08 (s, 3H, CH_3), 4.37 (s, 3H, CH_3), 7.57 (t, $J = 7.3$ Hz, 1H, H_7), 7.80 (t, $J = 7.3$ Hz, 1H, H_7), 7.92 (d, $J = 8.3$ Hz, 1H, H_8), 8.24 (d, $J = 7.1$ Hz, 1H, H_8), 8.38 (d, $J = 7.8$ Hz, 1H, H_4), 8.77 (dd, $J = 7.1$, 1.1 Hz, 1H, H_3), 9.81 (s, 1H, H_1); ^{13}C NMR (DMSO- d_6) δ : 30.32, 46.58, 107.04, 111.64, 119.35, 119.81, 121.75, 123.01, 129.51, 138.62, 139.32, 142.42, 145.46; HRMS (ESI) m/z calcd for $C_{13}H_{13}N_2$ $[M-I]^+$ 197.1079, found 197.1092.

γ -Carboline was prepared as described previously.³² The NMR spectrum was recorded on Bruker AV400 spectrometer. High resolution electrospray ionization (ESI) mass spectra were obtained on Bruker MicrOTOF II. The synthesis for the two cationic γ -carbolines was outlined in Fig. S1 of supplementary information. The characteristic data of **MPII**, 2-Methyl-2H-pyrido[4,3-b]indole and **DPII** have been shown in the part of spectroscopic data in supplementary information.

Materials

Calf thymus DNA (CT-DNA), Plasmid pBR322, Ethidium Bromide (EB) and Hoechst 33258 was purchased from Sigma-Aldrich. Reagents were of analytical grade from Sinopharm Chemical Reagent Co., Ltd unless specified otherwise. Double distilled and deionized water was used to prepare buffers, and ionic strength in buffers was adjusted with NaCl. The CT-DNA concentration in base pairs was determined by an extinction coefficient of $1.32 \times 10^4 M^{-1} cm^{-1}$ at 260 nm. The ratio $A_{260}/A_{280} > 1.80$ was used to confirm the high DNA purity. The DNA solution was stored for a short period of time at 4 °C if not used immediately.

A **MPII** stock solution (2×10^{-3} M) was prepared by dissolving an appropriate amount of **MPII** in double distilled and deionized water, and a **DPII** stock solution (2×10^{-3} M) was in double distilled and deionized water/DMSO (1:1).

Fluorescence experiments

Fluorescence spectra and titrations were measured on a Perkin-Elmer LS-55 spectrometer (Perkin-Elmer Co., USA) with Ex/Em slit 10 nm/10 nm. Fluorescence titrations were performed at a fixed cationic γ -carboline concentration (0.1 μM) with various concentrations of CT-DNA (0-10.2 μM) in the buffers with various ionic strengths. The fluorescence from 300 to 480 nm was recorded with Ex of 258 nm for **MPII**, and with Ex of 259 nm for **DPII**.

UV-Vis absorption spectra

UV-Vis absorption spectra and titrations were recorded on a Shimadzu UV-2600 spectrophotometer (Shimadzu Co., Japan). The spectrometric measurements were performed at room temperature in a quartz cuvette of 1 cm path length, and the sample solution was stirred for 3 min before measurement. UV-Vis absorption titration experiments were performed at a fixed cationic γ -carboline concentration (10 μM) with different CT-DNA concentrations (0-35.8 μM) in the buffers with various ionic strength. A reference cuvette contained corresponding

concentration of CT-DNA alone to nullify the absorbance of CT-DNA.

Circular Dichroism

CD spectra were recorded on a Jasco J-810 spectrometer (Tokyo, Japan). The CD spectra of CT-DNA (100 μM) in buffers with various ionic strengths and different concentrations (0, 10, 20 μM) of **MPII** and **DPII** were measured using a 1 cm path length cylindrical cell in the 220-320 nm wavelength region at room temperature. The bandwidth was 1 nm, and the response time was 1 s. Each spectrum was an average of three successive scans obtained by collecting data at 0.5 nm intervals at 100 nm/min scan rate with an appropriately corrected baseline.

EB/H33258 competitive experiments

CT-DNA solutions with EB in the different buffers were titrated by cationic γ -carbolines of increasing concentration (0-30 μM), with the constant concentrations of CT-DNA (5 μM) and EB (2 μM). After each addition of cationic γ -carboline, the fluorescent emission spectra of EB from 550 to 650 nm were recorded with Ex of 510 nm on a Perkin-Elmer LS-55 spectrometer with Ex/Em slit 10 nm/10 nm. The quenching percentage = $[F_{(EB-DNA)} - F_{(EB-DNA-compound)}] / [F_{(EB-DNA)} - F_{EB}]$.

A CT-DNA solutions with H33258 (CT-DNA/H33258 5 μM /2 μM) in the different buffers were prepared. The titrations were performed similar to EB competitive experiments by cationic γ -carbolines of increasing concentration (0-20 μM), where the fluorescent emission spectra of H33258 from 400 to 600 nm were recorded with Ex of 360 nm with Ex/Em slit 10 nm/5 nm. The quenching percentage = $[F_{(H33258-DNA)} - F_{(H33258-DNA-compound)}] / [F_{(H33258-DNA)} - F_{H33258}]$.

AFM experiments

The mixing mole ratios of the two cationic γ -carbolines and pBR322 base pairs were 0, 10:1 and 100:1. AFM experiments were performed as follows: take an aliquot of 10 μl mixture of cationic γ -carboline and pBR322 in 10^{-3} M buffer with 1mM $NiCl_2$ aqueous solution and deposit it on the newly cleaved mica surface directly. The deposited droplet was left on the mica surface for 3-5 min and unattached pBR322 was washed with MilliQ water. Gently the sample was dried under a stream of nitrogen. Finally, samples were scanned with tapping mode on a PicoScan 2500 PicoSPM II controller (Agilent, USA) with a silicon probe of $k = 40$ N/m and 300 kHz resonant frequency.

Conclusions

In this work, the DNA binding properties of cationic γ -carbolines were elucidated based on a series of experiments, and also the effect of ionic strength on cationic γ -carboline-DNA binding interaction was studied. Two cationic γ -carbolines were proved to strongly interact with DNA by intercalative binding. The γ -carboline **MPII** — with 2-N-methylpyridinium cation and 5-NH did not form a groove binding with DNA. However, another γ -carboline **DPII** with a methyl group substituting H atom at 5-NH of **MPII** showed stronger intercalative interaction to DNA than **MPII** did. The same binding modes and the different intercalative activities of **MPII** and **DPII** with DNA were decided by the similarity and difference in the structures between **MPII** and **DPII**. Planar and aromatic γ -carboline had a strongly intercalative interaction with DNA, while the dissociation of H from 5-NH of **MPII** resulted in a good water-solubility and less binding affinity to DNA. AFM images of pBR322 showed both **MPII** and **DPII** strongly interacted with DNA and induced conformational changes of DNA. Although

MPII showed less binding affinity to DNA, **MPII** caused DNA greater conformational change than **DPII** did.

Our studies also showed the interactions between cationic γ -carbolines and DNA were sensitive to ionic strength. The intercalation of cationic γ -carbolines into DNA would enhance the base stacking and make the positive Cotton effect increase correspondingly. With ionic strength increasing, the electrostatic repulsion between consecutive phosphate groups would decrease, and the base stacking would be more compact, which resulted in hardly intercalating of cationic γ -carbolines into DNA.

Acknowledgements

The authors are grateful for the financial supports of National Natural Science Foundation of China (NO. 21105114, 21002074).

Notes and references

^a School of Pharmaceutical Sciences, Wuhan University, Wuhan, Hubei 430072, PR China Fax: +86-27-68759850, E-mail: jjat@whu.edu.cn

^b Key Laboratory of Special Pathogens and Biosafety, Wuhan Institute of Virology, Chinese Academy of Sciences, Wuhan, Hubei 430071, PR

China Tel: +86-27-51861078, Email yujp@wh.iov.cn (Junping Yu) Wuhan, Hubei 430071, PR China Fax: +86-27-87199492, Email yujp@wh.iov.cn

† Electronic Supplementary Information (ESI) available: [synthesis and characterization of cationic γ -carbolines were included]. See DOI: 10.1039/b000000x/

‡ Footnotes should appear here. These might include comments relevant to but not central to the matter under discussion, limited experimental and spectral data, and crystallographic data.

- 1 T. Jia, J. Xiang, J. Wang, P. Guo and J. Yu, *Organic & Biomolecular Chemistry*, 2013, **11**, 5512-5520.
- 2 A. Gluszyńska, K. Bajor, I. Czerwińska, D. Kalet and B. Juskowiak, *Tetrahedron Letters*, 2010, **51**, 5415-5418.
- 3 A. Manna and S. Chakravorty, *The Journal of Physical Chemistry B*, 2012, **116**, 5226-5233.
- 4 R. Cao, W. Peng, Z. Wang and A. Xu, *Current Medicinal Chemistry*, 2007, **14**, 479-500.
- 5 N. J. Anderson, R. J. Tyacke, S. M. Husbands, D. J. Nutt, A. L. Hudson and E. S. J. Robinson, *Neuropharmacology*, 2006, **50**, 269-276.
- 6 M. M. Gonzalez, M. Vignoni, M. Pellon-Maison, M. A. Ales-Gandolfo, M. R. Gonzalez-Baro, R. Erra-Balsells, B. Epe and F. M. Cabrerizo, *Organic & Biomolecular Chemistry*, 2012, **10**, 1807-1819.
- 7 B. K. Paul and N. Guchhait, *The Journal of Physical Chemistry B*, 2011, **115**, 11938-11949.
- 8 H. Guan, X. Liu, W. Peng, R. Cao, Y. Ma, H. Chen and A. Xu, *Biochemical and Biophysical Research Communications*, 2006, **342**, 894-901.
- 9 Y. Funayama, K. Nishio, K. Wakabayashi, M. Nagao, K. Shimoi, T. Ohira, S. Hasegawa and N. Saijo, *Mutation Research/Fundamental and Molecular Mechanisms of Mutagenesis*, 1996, **349**, 183-191.
- 10 L. C. Tu, C.-S. Chen, I. C. Hsiao, J.-W. Chern, C.-H. Lin, Y.-C. Shen and S. F. Yeh, *Chemistry & Biology*, 2005, **12**, 1317-1324.
- 11 P. de Oliveira Figueiredo, R. T. Perdomo, F. R. Garcez, M. de Fatima Cepa Matos, J. E. de Carvalho and W. S. Garcez, *Bioorganic & Medicinal Chemistry Letters*, 2014, **24**, 1358-1361.
- 12 L. He, S.-Y. Liao, C.-P. Tan, R.-R. Ye, Y.-W. Xu, M. Zhao, L.-N. Ji and Z.-W. Mao, *Chemistry – A European Journal*, 2013, **19**, 12152-12160.
- 13 Y. Li, F. Liang, W. Jiang, F. Yu, R. Cao, Q. Ma, X. Dai, J. Jiang, Y. Wang and S. Si, *Cancer Biology & Therapy*, 2007, **6**, 1204-1210.
- 14 Y. Wang, Q. Jin, G. Lin, T. Yang, Z. Wang, Y. Lu, Y. Tang, L. Liu and T. Lu, *Chemical and Pharmaceutical Bulletin*, 2012, **60**, 435-441.
- 15 X. Han, J. Zhang, L. Guo, R. Cao, Y. Li, N. Li, Q. Ma, J. Wu, Y. Wang and S. Si, *PLoS ONE*, 2012, **7**, 1-11.
- 16 J. Zhang, Y. Li, L. Guo, R. Cao, P. Zhao, W. Jiang, Q. Ma, H. Yi, Z. Li, J. Jiang, J. Wu, Y. Wang and S. Si, *Cancer Biology & Therapy*, 2009, **8**, 2374-2383.

- 17 M. M. Gonzalez, M. Pellon-Maison, M. A. Ales-Gandolfo, M. R. Gonzalez-Baro, R. Erra-Balsells and F. M. Cabrerizo, *Organic & Biomolecular Chemistry*, 2010, **8**, 2543-2552.
- 18 A. Molina, J. J. Vaquero, J. Garcia-Navio, J. Alvarez-Builla, M. M. Rodrigo, O. Castaño and J. de Andres, *Bioorganic & Medicinal Chemistry Letters*, 1996, **6**, 1453-1456.
- 19 T. Jia, Z.-X. Jiang, K. Wang and Z.-Y. Li, *Biophysical Chemistry*, 2006, **119**, 295-302.
- 20 Y. R. Kim, L. Gong, J. Park, Y. J. Jang, J. Kim and S. K. Kim, *The Journal of Physical Chemistry B*, 2012, **116**, 2330-2337.
- 21 Y. G. Sun, D. Sun, W. Yu, M. C. Zhu, F. Ding, Y. N. Liu, E. J. Gao, S. J. Wang, G. Xiong, I. Dragutan and V. Dragutan, *Dalton Transactions*, 2013, **42**, 3957-3967.
- 22 V. I. Ivanov, L. E. Minchenkova, A. K. Schyolkina and A. I. Poletayev, *Biopolymers*, 1973, **12**, 89-110.
- 23 J.-H. Tan, Y.-j. Lu, Z.-S. Huang, L.-Q. Gu and J.-Y. Wu, *European Journal of Medicinal Chemistry*, 2007, **42**, 1169-1175.
- 24 S. Y. Breusegem, R. M. Clegg and F. G. Loontjens, *Journal of Molecular Biology*, 2002, **315**, 1049-1061.
- 25 N. K. Modukuru, K. J. Snow, B. S. Perrin, J. Thota and C. V. Kumar, *The Journal of Physical Chemistry B*, 2005, **109**, 11810-11818.
- 26 K. Klemm, M. Radić Stojković, G. Horvat, V. Tomišić, I. Piantanida and C. Schmuck, *Chemistry – A European Journal*, 2012, **18**, 1352-1363.
- 27 Y. Jiang, C. Ke, P. A. Mieczkowski and P. E. Marszalek, *Biophysical Journal*, 2007, **93**, 1758-1767.
- 28 W. Vanderlinden, M. Blunt, C. C. David, C. Moucheron, A. Kirsch-De Mesmaeker and S. De Feyter, *Journal of the American Chemical Society*, 2012, **134**, 10214-10221.
- 29 F. A. Tanius, D. Ding, D. A. Patrick, R. R. Tidwell and W. D. Wilson, *Biochemistry*, 1997, **36**, 15315-15325.
- 30 F. A. Tanius, D. Ding, D. A. Patrick, C. Bailly, R. R. Tidwell and W. D. Wilson, *Biochemistry*, 2000, **39**, 12091-12101.
- 31 A. P. Gray, *Journal of the American Chemical Society*, 1955, **77**, 5930-5932.
- 32 K. Sako, H. Aoyama, S. Sato, Y. Hashimoto and M. Baba, *Bioorganic & Medicinal Chemistry*, 2008, **16**, 3780-3790.